Study of the photocatalytic oxidation mechanism of 1,3-dihydroxyanthraquinone using DFT methodology

Carlos M. Cortés-Romero[*], Elba Ortiz[**], A. Cuán[*], Hugo Solís[**]
[*]Ingeniería en Nanotecnología, Universidad Autónoma de Querétaro.
Carretera a Chichemequillas, Ejido Bolaños, Querétaro, Qro. 76140. México.
carloscort2001@yahoo.com.mx; angelescuan24@yahoo.com.mx.
[**]Área de Química y Fiscoquímica Ambiental,Ciencias Básicas,Universidad Autónoma Metropolitana-Azcapotzalco, Av. San Pablo 180, México D.F. 02200, México.
mariaelbaortiz@gmail.com; hsoliscorrea@yahoo.com.mx

ABSTRACT

The structural stability of 1,3,-dihydroxyanthraquinone (purpuroxanthin vegetal dye) has been theoretically studied toward a better understanding of the chemical reactivity of this molecule and its intermediates formed during the photocatalytic oxidation. During this process, oxidizing species such as hydroxyl and oxyhydryl (•OH, HO2•) as well as oxygen and ozone free radical (O2-• and O3-•) are the keystone for the reaction to occur. By performing DFT calculations, under restricted calculation or assuming opening of the shell for the radical systems, vibrational frequencies were obtained for all the stationary states at the same level of theory. Corrections for zero-point energy (ZPE) and thermochemistry were also taken into account for the reaction coordinate pathways. Moreover, the IR spectrum and the vibrational frequencies and the molecular emission energy (UV spectrum) were calculated. The UV spectrum was obtained with vertical transition energy of the lowest singlet excited state by means the time-depending DFT (TDDFT).

Keywords: 1,3-dihydroxyanthraquinone, photocatalytic oxidation, IR spectrum, UV-Vis spectrum, DFT.

1 INTRODUCTION

Polynuclear molecules related to 9,10-anthraquinone derivatives are commonly used either from therapeutic point of view or for industrial applications. For instance, purpurine (1,2,4-trihydroxyanthraquinone) has anticancer, anti-inflammatory, antifungal, and antioxidant activity [1]. The dihydroxyderivatives from anthraquinone, such as alizarin, purpuroxanthin, etc., can be used as additive for coloring food or as a pigment for various products such as textile [2]. The case of 1,3,-dihydroxyanthraquinone (purpuroxanthin dye) is quite interesting due to its inherent properties that makes it useful in medical application as well as for the aforementioned textile dye use. However, the presence of this molecule and other related dyes in water wasted from textile industry makes it an environmental problem due to the incessant and non-controlled poisoning of aquatic animals and plants [3]. This is the reason of searching an environmental-friendly process aimed at degrading or mineralizing those dyes and its potential product intermediates. Photocatalytic oxidation is one of the advanced oxidation processes (AOP´s) which can be used for this purpose. In short, the photocatalytic process involves the presence of a substance (catalyst) that enhances the formation of the oxidant species by means of photonic stimuli. In this work, the structural stability of the purpuroxanthin molecule has been studied by quantumchemical calculations to gain insight in the funtamental behavior of the molecule by calculating the electronic properties and the mechanistic study of the hydroxyl (•OH) radical-initiated oxidation of pupuroxanthin dye, in gas phase. All possible reaction pathways were considered as well as the IR and UV spectrum theoretically computed.

2 METHODOLOGY

The electronic structure calculations were performed with the Gaussian 09 program package, within the density functional theory scheme [3]. The M05-2X functional and the 6-311++g(d,p) bases were suitable for our current aim. Unrestricted calculations were assumed for open shell systems, i.e, for radical systems case. Vibrational frequency calculations were performed for all the stationary states at the same level of theory to identify the local minima and transition states by the number of imaginary frequencies, for the transition states (only one imaginary frequency) and cero for the local minima. Zero-point energy (ZPE) and thermochemistry corrections are also taken into account, for the reaction coordinate pathways. The IR spectrum and the vibrational frequencies and the molecular emission energy (UV spectrum) were calculated. The UV spectrum was obtained with vertical transition energy of the lowest singlet excited state by means the time-depending DFT (TDDFT) [4].

3 RESULTS

3.1 1,3-dihydroxyanthraquinone molecule

The most stable conformation for the 1,3-dihydroxyanthraquinone molecule (PPX), M05-2X/6311++G(d,p) in gas phase is showed in the Figure 1. The optimized geometry shows a planar structure for the molecule, which include the hydroxyl grups also oriented en the same plane of the aromatic rings by stabilization of intramolecular interactions between the oxygen (O19) from the carbonyl group and the hydrogen atom (H18) from the –OH group, i.e., the lone pair–antibonding orbital interactions between the carbonyl oxygen and the adjacent OH bond is responsible for hydrogen bond interaction given a strongest stabilizing effect; this is in line with literature reported [5].

An exploration of its electronic distribution was investigated to gain insight in the fundamental behavior. Then the HOMO-LUMO frontier orbitals where calculated, see Figure 2. The red and green colors represent the positive and negative phases, respectively. It can be observed that both frontier orbitals show bonding and antibonding character. The HOMO is characterized by carbon-carbon (-C=C-) bonding and hydroxyl (-OH) bonding, while C6, C8 and C11 do not participate in the HOMO distribution. For the LUMO π* orbital several bonding and antibonding regions are observed along the framework rings including all the antibonding π* oxygen's, while the hydrogens atoms do not participate.

The potential electronic surface (PES) was also investigated and it is showed in the Figure 3. According to the colours code, it comes from red to blue, where red corresponds to zones with highest electronic density and blue the lowest electronic density, then yellow colour corresponds to to high electronic density. Then the PES distribution in the PPX shows that the oxygens from the carbonyl and from the hydroxyls groups and the hydrogens atoms with coloring with light blue are zones with lower electronic density, while the atom hydrogens (H16 y H18) shows the lowest electronic density wich can be related with certain acidity character, in fact the atomic charge distribution in the molecule is 0.29 y 0.32 while for the rest of the hydrogen atoms are ranged about 0.18-0.23 e^-. Refering the rest of the -C=C- framework the charge distribution is negative for all the carbons links to oxygens and also for the C7, C9 y C10; while for the rest possitive charged. This distribution gives preferential radical attack •OH or radical addition.

IR Spectra. The IR spectra was calculated according to the vibrational frequencies and absorption bands, for the PPX and it is analyzed to determine the main characteristics like high –OH vibrational frequencies 3400 and 3500 cm^{-1}, which indicates a higher susceptibility of these groups to reacts or to modify the electronic density of the –C=C– neighbor site.

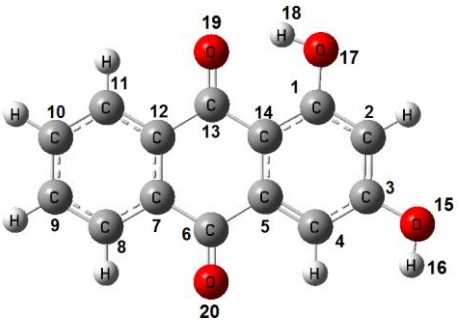

Figure 1. Optimized structe for the PPX.

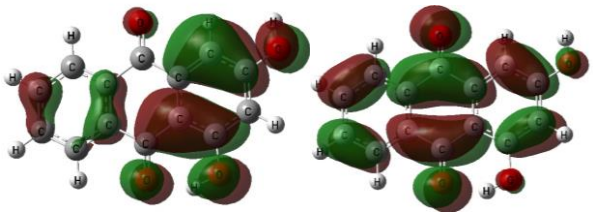

a) HOMO b) LUMO

Figure 2. Frontier orbitals for the PPX.

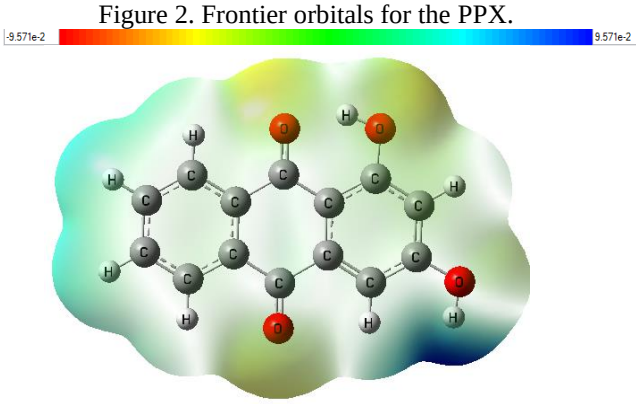

Figure 3. Schematic potential electronic surface (PES) for the PPX. The PES is proyected within the electronic density. At the botton is the colour code from highest to lowest electronic density.

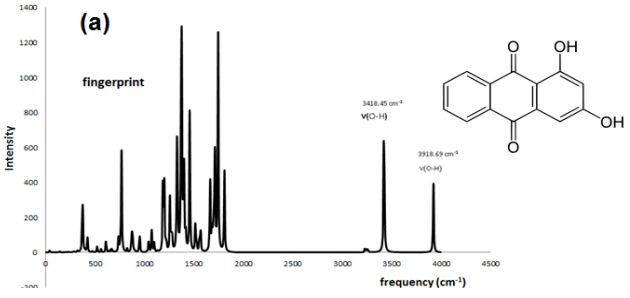

Figure 4. Theoretical spectrum of IR for PPX.

UV−Vis Spectra. After geometry optimization, TD-DFT calculations for singlet excitations were carried out to

obtain the UV/VIS spectra of the PPX molecule. In order to compare our results with those obtained in the experiments, we added the sovent effect (water) by using the polarizable continuum model of solvation (SMD-PCM) [6]. The molecular stabilization energy of the PPX reaches 52.3 kJ/mol with water is taking into account as solvent with respect to in vacuo conditions.The excitations that are responsible for the color present a $\pi-\pi^*$ character with a large oscillator strength. From the Figure 5, theoretical coloring band is ranged between 321-457.55 which the principal contribution is given by HOMO –> LUMO excitation. The reported λmax corresponds to the transition energy from the ground electronic state to the first dipole-allowed excited state.

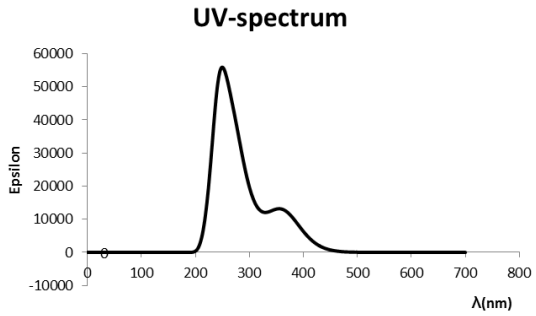

Figure 5. Theoretical spectrum of UV-Vis for PPX.

3.2 •OH radical addition

Only the •OH radical attack was consider to carbon atoms, hydrogen abstraction were not consider at this time. Then, there are fourteen possible •OH radical attack or in this case, •OH addition were consider. For this study the calculations correpond to phase gas only, the effect solvent is not yet finish. The corresponding transtions states (TS) and adduct (like products) were obtained following the possible ruts or reactions channels. Hence, •OH addition - type pathways that correspond to the radical oxygen atom binding to any carbon atom in the molecule. Given that PPX molecule is planar, reaction from above or below the plane leads to equivalent products. The Relative electronic energies (including ZPE) and Gibbs free energies (including thermodynamic corrections) are calculated with respect to the sum of the separated reactants (PPX + •OH) and they are reported in Table 1. In this table, ΔE corresponds to $\Delta E = E_{RC} - E_R$, where E_{RC} is the prereactive complex stabilization energy (adduct formation). Analogously, $\Delta G = G_{RC} - G_R$, is the prereactive complex stabilization Gibbs free energy. $\Delta E^{\ddagger}$ and $\Delta G^{\ddagger}$ are the energy and Gibbs free energy of the transition state relative to reactants, and ΔE and ΔG are the reaction energy and reaction Gibbs free energy. Then analysing the Table data, the most viable attach of the •OH radical species is for C4, which not energetic barrier is found for $\Delta E^{\ddagger}$ but this is corrected by Gibbs free energies. Even so, this rute has less energetic cost no matter $\Delta E^{\ddagger}$ and $\Delta G^{\ddagger}$ are taken into account and the prereactive complex is the most stabilized species, see Figure 6. This prereactive species point out to the purpurin colorant formation before a degradation or destabilization could be carried out. All the •OH addition are viable according to the energetic barriers, except for C1, C3, C6, C13 y C14 due to the high value of barriers for the TS formation.

All the vibrational imaginary frequency for each TS corresponds to the vertical movement of the •OH group in the direction of the carbon sites, as an example is shown In the Figure 6a for the •OH radical attack to carbon atom, C4.

All additions occur in a similar way and modify the aromaticity of the molecule because the C atom at the reaction site changes from an sp^2 to sp^3 hybridization. As a result adducts are not completely planar.

•OH addition	$\Delta E^{\ddagger}$	ΔE	$\Delta G^{\ddagger}$	ΔG
C1	----	----	----	----
C2	0.80	-105.38	36.57	-67.77
C3	----	----	----	----
C4	-12.01	-148.48	23.48	-110.87
C5	11.86	-61.51	49.79	-23.36
C6	37.53	-42.49	76.34	3.19
C7	11.86	-54.21	49.79	-15.68
C8	8.83	-54.61	44.12	-46.22
C9	9.23	-54.47	44.23	-46.12
C10	8.98	-82.62	44.29	-46.05
C11	8.76	-87.63	43.83	-49.81
C12	11.64	-52.04	48.86	-15.47
C13	51.36	-28.66	89.64	16.50
C14	49.02	-31.00	200.04	6.99

Table 1: Relative Electronic Energies (Including ZPE) and Gibbs Free Energies (Including Thermal Correction Energy at 298 K), in kJ/mol, in the •OH-Addition to carbon´s PPX molecule.

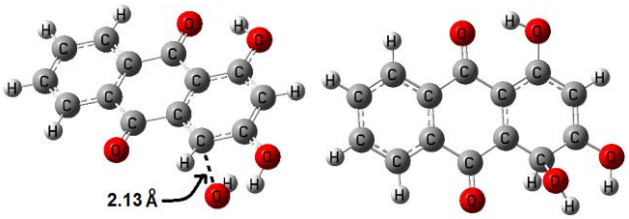

a) TS-PPX-OH• b) Aducct-PPX-OH•

Figure 6. a) Stationary points for the Transition State. The vibrational imaginary frequency corresponds to the •OH radical attack to carbon atom, C4; b) Adduct structure as a result of the •OH-addition to the carbon atom, C4.

4 CONCLUSIONS

The mechanism of oxidation of purpuroxanthin dye by the photocatalytic oxidation was supported by quantum chemical DFT calculations. The reactivity of this dye molecule dye by reaction with hydroxyl radicals (•OH) under atmospheric oxidative conditions was evaluated assuming oxidant addition at preferred sites. All reaction pathways were considered, and all stationary points were characterized. The preferential •OH radical addition was for the C4 pointing out to the purpurin colorant formation as one of the reaction products. The calculated $\Delta G^{\ddagger}$ barrier was 23.48 kJ/mol stabilizing the additon by 110.87 kJ/mol with respect to the reactives species. For the carbons C2, C5, C7 to C12 the $\Delta G^{\ddagger}$ barriers were ranged among 36 to 49 kJ/mol the adducts were stabilized 16 kJ/mol for C7, C12 and about 50 kJ/mol for the C8 to C11, while for C3 was ranged about 68 kJ/mol. As more higher is the $\Delta G^{\ddagger}$ barrier less stability was obtained for the prereactive complex.
For the viable routes of the reaction coordinate the reactions are exothermic. The theoretical IR calculated shows that –OH vibrational frequencies are about 3400 and 3500 cm^{-1}, which indicates a higher susceptibility of these groups to reacts, in fact the hydrogens atoms from the –OH groups present certain acidity. And for the UV-Vis, the band found ranged between 321-457.55 which the principal contribution is given by HOMO –> LUMO excitation.

5 ACKNOWLEDGMENTS

Autors acknowledges financial support for this work to CONACYT through project No. Project 153663 CB-2010-01 and also to the computer time from Laboratorio de Visualización y Cómputo Paralelo at Universidad Autónoma Metropolitana-Iztapalapa and Dirección General de Cómputo.

REFERENCES

[1] Pérez-Garrido A., Morales-Helguera A., Morillas Ruiz J. M., Zafrilla-Rentero P. European Journal of Medicinal Chemistry 49, 86-94, 2012.
[2] Drivas I., Blackburn R. S., RaynerC. M. Dyes and Pigments 88, 7-17, 2011.
[3] Ashis Kumar Samanta and Adwaita Konar. Dyeing of Textiles with Natural Dyes, Natural Dyes, Dr. Emriye Akcakoca Kumbasar (Ed.), ISBN: 978-953-307-783-3, InTech, 2011. Available from: http://www.intechopen.com/books/natural-dyes/dyeingof textiles-with-natural-dyes
[4] M. J. Frish, et al. Gaussian 09, Revision v.01; Gaussian, Inc. Pittsburg, PA (2009).
[5] S. R. Jeremic, S. F. Sehovic, N. T.. Manojlovic´ and z. s. Markovic´, Monatsh Chem (2012) 143,427–435, 2012.
[6] Cammi R, Mennucci B, Tomasi J J Phys Chem A. 104, 5631,2000.